Available online at www.sciencedirect.com

ScienceDirect

Journal of the Franklin Institute 354 (2017) 6831–6854

www.elsevier.com/locate/jfranklin

Dual boundary conditional integral backstepping control of a twin rotor MIMO system

A. Haruna[a,b], Z. Mohamed[a,*], M.Ö. Efe[c], Mohd Ariffanan M. Basri[a]

[a] *Faculty of Electrical Engineering, Universiti Teknologi Malaysia, 81310 UTM Johor Bahru, Johor, Malaysia*

[b] *Department of Mechatronics Engineering, Faculty of Engineering, Bayero University Kano, PMB 3011, Kano, Nigeria*

[c] *Department of Computer Engineering, Hacettepe University, 06800 Ankara, Turkey.*

Received 13 February 2017; received in revised form 16 July 2017; accepted 30 August 2017
Available online 5 September 2017

Abstract

Conditional integration is a technique used to improve the transient performance of controllers with integral action. This paper proposes a novel modification of this technique and integral backstepping for the control of a Twin Rotor MIMO System (TRMS) to ensure efficient asymptotic output regulation of the system without degrading the transient response. The control objectives are to stabilize the helicopter-like system, reach a desired position and precisely track a given trajectory in the presence of significant cross couplings. The TRMS is decoupled into the vertical subsystem (VS) and the horizontal subsystem (HS) and an integral backstepping controller (IBC) is designed for each subsystem with the cross couplings considered as uncertainties. An adaptable integral gain law, which can be applied to any continuous control law, is then formulated to provide integral action conditionally within two (outer and inner) boundary layers, based on the output tracking error and reference signals. Simulation results show that the obtained dual boundary conditional integral backstepping control (DBCIBC) approach achieves robust output regulation in the presence of the system's uncertainties and external disturbances whilst maintaining a good transient response. Furthermore, comparisons with three available methods in the literature also indicate that the DBCIBC significantly improves performance in terms of error and control signal indices especially for the case of tracking a time varying reference input where the error index in the VS is reduced by over 50% on an average.

* Corresponding author.
E-mail address: zahar@fke.utm.my (Z. Mohamed).

http://dx.doi.org/10.1016/j.jfranklin.2017.08.050

1. Introduction

The TRMS which in many ways resembles a helicopter albeit with less degrees of freedom (DOFs), exemplifies a high-order nonlinear cross-coupled under-actuated system [1] and has attracted interest from researchers in recent years. The control objective is to make the beam of the TRMS track a predetermined trajectory quickly by accurately positioning its HS (yaw) and VS (pitch) angles in the presence of significant cross couplings. Several investigations into achieving this objective have been reported. Juang et al. [2] examined the use of four PID controllers with independent inputs for control of the system. The parameters of the controllers were obtained by a modified method of a real-type genetic algorithm (M-RGA) with a performance index as a fitness function. An augmented control scheme consisting of a 4-impulse feedforward controller and two PID feedback compensators [3] and a robust PID-based deadbeat control technique [4] have also been proposed for the system. PID control of high order systems however often leads to oscillations resulting in slower settling times as the results in [2–4]. In [5], an optimal LQG compensator augmented with feedforward control was designed to reduce vibrations for the pitch subsystem in 1-DOF. Linear optimal controllers like LQR [6] and LQR with integral action [7] have also been suggested for step reference inputs. Application of nonlinear Model Predictive Control to the system is reported in Rahideh and Shaheed [8] where the nonlinear model had to be adaptively linearized during the prediction horizon. Intelligent controllers employing fuzzy logic were proposed in [9,10]. The number of rules is however large which motivated the parallel distributed fuzzy LQR in [11] with results given only for fixed reference inputs.

Variants of the SMC scheme have also been designed for the system [12–14]. A Fuzzy Sliding Fuzzy Integral Sliding Controller (FSFISC) was proposed by Tao et al. [15] while an adaptive second order SMC (SOSMC) was suggested in Mondal and Mahanta [16]. Although the results were shown to be better than the PID in [2], the control laws for the FSFISC and SOSMC are however quite complex and the precision of tracking time varying waveforms could be improved. Other nonlinear controllers suggested for the system include H-infinity [17], feedback linearisation [18,19] and quasi-Linear Parameter Varying (LPV) control [20] where a high fidelity model of the TRMS had first to be transformed into a discrete time polytopic quasi-LPV model.

With the exception of the PID based controllers, the methods proposed for the TRMS seem to apply integral control (with low gain) only to the pitch subsystem of the TRMS. The suspected reason being that although integral action can be introduced to achieve output regulation of both linear and nonlinear systems in the presence of parameter uncertainties and/or constant external disturbances [21,22], it has the drawback of deteriorating the transient performance. Undesirable overshoot and oscillations in the closed loop which can also lead to longer settling times are well-known problems associated with integral control. Integral action must therefore be applied with caution.

To alleviate these problems, the integrator is modified in [23] to provide integral action conditionally i.e. within a specific boundary in a Sliding Mode Control (SMC) framework and extended to a general class of state feedback controllers in [24] using a Lyapunov redesign approach. More recently, a variable gain integral controller has been applied to solve this problem in linear plants [25]. It is thus envisaged that the transient performance and precision tracking of constant or time varying waveforms for both HS and VS of the TRMS can be significantly improved upon by appropriately applying a suitable controller with an appropriate integration method.

Backstepping is a natural choice for the control of the TRMS as the system is nonlinear, under-actuated and triangular. That is, the system's un-actuated states are controlled by the interaction with the system's actuated states in a cascaded manner. The most common and widely used method of including integral action in backstepping is to use parameter adaptation [26,27]. Parameter update laws however significantly complicate the control computation and are also well-known to degrade the transient performance when adaptation is initiated. A relatively straight-forward approach introduced in [28] includes integral action by augmenting the first step of the backstepping design with an integral of the output error. This method of integral backstepping has been very recently proposed for the Two Rotor Aero-dynamical System (a variant of the TRMS) in [29]. The proposed controller uses command filtered compensation (where virtual backstepping control derivatives are generated using low pass filters) which can further degrade transient performance and robustness. The robustness of the proposed method was improved by further augmenting the integral backstepping controller with a disturbance observer.

In this paper, a modified dual boundary conditional integral backstepping controller (DBCIBC) with analytical virtual control derivatives is proposed for the TRMS to achieve asymptotic regulation of the output to a bounded constant or time varying reference signal without degrading the transient performance. The main contribution of this work is the formulation of an adaptation law which can be applied to a general class of controllers with a continuous control law, to provide integral action conditionally within two (outer and inner) boundary layers in order to improve tracking ability and robustness whilst maintaining a good transient response. This is achieved not only by providing integral action conditionally within the specified boundaries, but also by modification of the integral law within the inner boundary layer to provide integral action with a continuous variable gain based on the reference signal and tracking error. The resulting control law thus has some adaptation capability, thereby improving robustness during the transient phase and allowing use of sufficiently large integral gains in the case of a sinusoidal reference input after the transient period to further minimise the tracking error. The method avoids the added complexity of designing a disturbance observer or use of internal model control and also solves the problem of tracking associated with integral backstepping control where the integrator appears at the first step of the backstepping design as highlighted in [26]. It is demonstrated that an integral backstepping controller with analytical virtual control derivatives and a saturated integrator (with a sufficient gain) significantly improves tracking of constant and sinusoidal waveforms while preserving the robustness properties of the system. Furthermore, this study compares the performance of the DBCIBC with that of the M-RGA optimised PID controller proposed for the system in [2], the FSFISC in [15] and the SOSMC in [16]. The remainder of this paper is organised as follows. A model description of the TRMS is provided in Section 2. The integral backstepping controller is designed in Section 3. In Section 4, the dual boundary conditional integral law is introduced. The stability of the system under the proposed control approach is analysed in Section 5. Simulation results are provided in Section 6 and concluding remarks are given at the end of the paper.

2. Model description of the TRMS

The TRMS shown in Fig. 1 consists of a beam pivoted at its base. The articulated joint allows the beam to rotate in such a way that its ends move on the horizontal (yaw) and vertical (pitch) planes. The main and tail rotors are driven by DC motors and attached to the ends of the beam. A counterbalance arm with a weight at its end is fixed to the beam at the

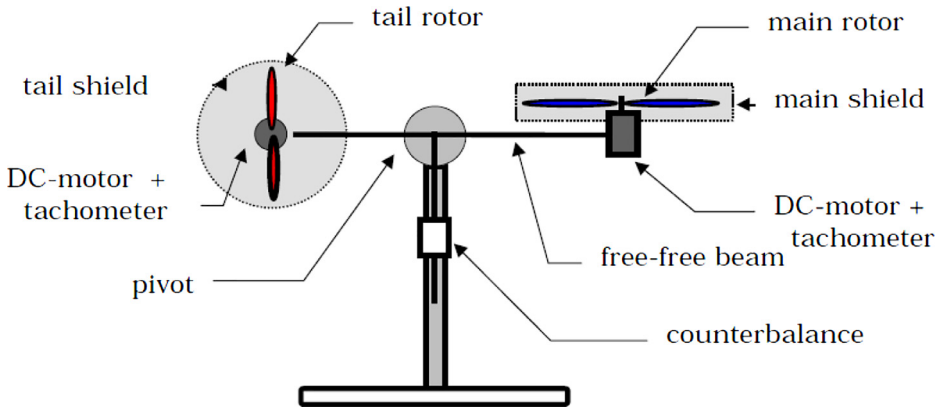

Fig. 1. TRMS component parts [1].

Table 1
TRMS physical parameters [1].

Symbol	Description	Value
l_t	Length of the tail part of the beam	0.25 m
l_m	Length of the main part of the beam	0.236 m
k_h	friction constant of the tail propeller subsystem	0.0054
k_v	friction constant of the main propeller subsystem	0.0095
J_{tr}	Moment of inertia for the tail rotor	1.6543×10^{-5} kgm^2
J_{mr}	Moment of inertia for the main rotor	2.65×10^{-5} kgm^2
T_{tr}	time constant of the tail rotor	0.3842 s
T_{mr}	Time constant of the main rotor	1.432 s
S_f	Balance scale	8.4332×10^{-4}
A	Mechanical constant	0.0947
B	Mechanical constant	0.1086
C	Mechanical constant	0.0117
D	Mechanical constant	0.0016
E	Mechanical constant	0.0490
F	Mechanical constant	0.0062
g	Gravitational acceleration	9.81 ms^{-2}
J_v	Sum of moments of inertia relative to the horizontal axis	0.1099

pivot. The system is balanced in such a way that when the motors are switched off, the main rotor end of the beam is lowered. Unlike conventional helicopters where aerodynamic thrust is generated by changing the angles of attack of the propellers, aerodynamic thrust in the TRMS is generated by increasing the rotation speed of the rotors. The result is a complex, high order nonlinear system with significant cross couplings i.e. each rotor affects both position angles. An approximate Newtonian mathematical model of the TRMS is obtained by using Newton's second law of motion and converted into state-space form [1] as expressed in Eq. (1) with the description and values of the physical parameters provided in Table 1.

$$\dot{x}_1 = x_3$$
$$\dot{x}_2 = x_4$$

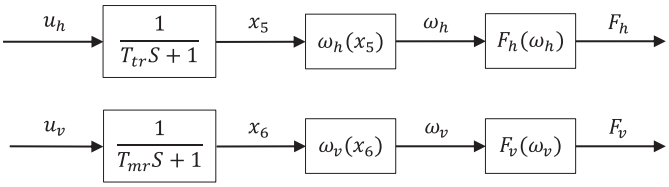

Fig. 2. Relationships between the input voltages, armature currents, rotor speeds and propulsive forces in the tail and main rotors [1].

$$\dot{x}_3 = \frac{1}{J_h}\Bigg[l_t S_f F_h(x_5)\cos x_2 - k_h x_3 + x_3 x_4 (D-E)\sin(2x_2) - J_{mr}\omega_v(x_6)x_4 \sin x_2 + \frac{J_{mr}}{T_{mr}}(u_v - x_6)\frac{d\omega_v(x_6)}{dx_6}\cos x_2\Bigg]$$

$$\dot{x}_4 = \frac{1}{J_v}\Bigg[l_m S_f F_v(x_6) - k_v x_4 + g((A-B)\cos x_2 - C\sin x_2) - 0.0252{x_3}^2 \sin(2x_2) + \frac{J_{tr}}{T_{tr}}(u_h - x_5)\frac{d\omega_h(x_5)}{dx_5}\Bigg]$$

$$\dot{x}_5 = \frac{1}{T_{tr}}(u_h - x_5)$$

$$\dot{x}_6 = \frac{1}{T_{mr}}(u_v - x_6) \tag{1}$$

where x_1 and x_2 are the yaw and pitch angles, respectively, of the beam, x_3 and x_4 are the angular velocities of the beam around the horizontal and vertical axes, respectively, u_h is the input voltage to the tail rotor, x_5 is the tail rotor armature current, u_v is the input voltage to the main rotor and x_6 is its armature current, ω_h is the rotation speed of the tail rotor and F_h is the propulsive force it generates, ω_v is the speed of the main rotor and F_v is its propulsive force.

The sum of moments of inertia relative to the vertical axis J_h is dependent on the pitch position (x_2) of the beam and can be expressed as:

$$J_h = D\,\sin^2 x_2 + E\cos^2 x_2 + F \tag{2}$$

The input voltage signals to the motors are normalised and change in the range -1 to $+1$ which corresponds to a voltage range of ± 5 V. The nonlinear relationships between the armature current and rotational speed as well as the rotational speed and thrust (Fig. 2) generated by both rotors are determined experimentally and approximated by Eqs. (3)–(6).

$$\omega_h(x_5) \approx 2020{x_5}^5 - 194.69{x_5}^4 - 4283.15{x_5}^3 + 262.27{x_5}^2 + 3768.83x_5 \tag{3}$$

$$F_h(\omega_h) \approx -3\times 10^{-14}{\omega_h}^5 - 1.595\times 10^{-11}{\omega_h}^4 + 2.511\times 10^{-7}{\omega_h}^3 - 1.808\times 10^{-4}{\omega_h}^2 + 8.01\times 10^{-2}\omega_h \tag{4}$$

$$\omega_v(x_6) \approx 90.99{x_6}^6 + 599.73{x_6}^5 - 129.26{x_6}^4 - 1238.64{x_6}^3 + 63.45{x_6}^2 + 1283.41x_6 \tag{5}$$

$$F_v(\omega_v) \approx -3.48\times 10^{-12}{\omega_v}^5 + 1.09\times 10^{-9}{\omega_v}^4 + 4.123\times 10^{-6}{\omega_v}^3 - 1.632\times 10^{-4}{\omega_v}^2 + 9.544\times 10^{-2}\omega_v \tag{6}$$

The model introduced above shows a set of coupled and nonlinear dynamical relations between the state variables involved. This is a prime challenge to address in the control design process.

3. Integral backstepping controller design

The controller design is presented in this section through application of the iterative backstepping design procedure to the TRMS by considering the cross couplings between the HS and VS as uncertainties. The integral of the error is added to the first stabilising function in the iterative backstepping design to introduce integral action in order to eliminate steady state error and improve disturbance rejection [28,30]. A detailed description of the iterative backstepping design process can be found in [31,32].

3.1. Horizontal subsystem integral backstepping

The decoupled model of the HS of the TRMS is expressed as [1]

$$\begin{aligned}\dot{x}_1 &= x_3\\ \dot{x}_3 &= \frac{1}{J_h}\left[l_t S_f F_h(x_5)\cos x_2 - k_h x_3\right]\\ \dot{x}_5 &= \frac{1}{T_{tr}}(u_h - x_5)\end{aligned} \tag{7}$$

Define

$$z_1 := x_1 - x_{1d} \tag{8}$$

$$z_3 := x_3 - \alpha_1 \tag{9}$$

$$z_5 := F_h(x_5) - \alpha_3 \tag{10}$$

where x_{1d} is the desired yaw angle and α_1 and α_3 are stabilising functions yet to be determined.

Step 1:

Select a Control Lyapunov function (CLF) as

$$V_1 = \frac{\lambda_1}{2}{\chi_1}^2 + \frac{1}{2}{z_1}^2 \tag{11}$$

where $\chi_1 = \int_0^t z_1(\tau)d\tau$ and λ_1 is a positive constant.

Therefore,

$$\dot{V}_1 = \lambda_1\chi_1\dot{\chi}_1 + z_1\dot{z}_1 = \lambda_1\chi_1 z_1 + z_1(\dot{x}_1 - \dot{x}_{1d}) = \lambda_1\chi_1 z_1 + z_1(x_3 - \dot{x}_{1d}) \tag{12}$$

By taking x_3 as the virtual control, a stabilising function $\alpha_1(x_1)$ for z_1 is designed as

$$\alpha_1(x_1) = -c_1 z_1 - \lambda_1\chi_1 + \dot{x}_{1d}, c_1, \lambda_1 > 0 \tag{13}$$

Hence,

$$\dot{V}_1 = -c_1{z_1}^2 \tag{14}$$

Step 2:

Select a CLF

$$V_3 = \frac{\lambda_1}{2}{\chi_1}^2 + \frac{1}{2}{z_1}^2 + \frac{1}{2}{z_3}^2 \tag{15}$$

Its derivative is

$$\dot{V}_3 = \lambda_1 \chi_1 \dot{\chi}_1 + z_1 \dot{z}_1 + z_3 \dot{z}_3 \tag{16}$$

The resultant dynamics of z_1 is obtained as

$$\dot{z}_1 = x_3 - \dot{x}_{1d} = x_3 - \alpha_1 + \ \alpha_1 - \dot{x}_{1d} \tag{17}$$

$$\dot{z}_1 = z_3 - c_1 z_1 - \lambda_1 \chi_1 \tag{18}$$

With $\dot{z}_3 = \dot{x}_3 - \dot{\alpha}_1(x_1)$, the dynamics of z_3 is expressed as

$$\dot{z}_3 = \frac{1}{J_h}\left[l_t S_f F_h(x_5)\cos\ x_2 - k_h x_3\right] - \frac{\partial \alpha_1}{\partial x_1}\dot{x}_1 \tag{19}$$

By substituting Eqs. (18) and (19) into Eq. (16), $\dot{V}_3$ is obtained as

$$\dot{V}_3 = -c_1 {z_1}^2 + z_3\left[z_1 + \frac{l_t S_f}{J_h}(F_h(x_5)\cos\ x_2) - \frac{1}{J_h}(k_h x_3) - \frac{\partial \alpha_1}{\partial x_1}\dot{x}_1\right] \tag{20}$$

Taking $F_h(x_5)$ as the virtual control, design $\alpha_3(x_1, x_3)$ as

$$\alpha_3(x_1, x_3) = \frac{J_h}{l_t S_f \cos\ x_2}\left[-z_1 + \frac{1}{J_h}(k_h x_3) + \frac{\partial \alpha_1}{\partial x_1}\dot{x}_1 - c_3 z_3\right] \tag{21}$$

So that,

$$\dot{V}_3 = -c_1 z_1^2 - c_3 z_3^2, \quad c_1, c_3 > 0 \tag{22}$$

Step 3:

Finally, the full state control input u_h to stabilize the entire horizontal subsystem is designed.

Select a CLF as

$$V_5 = \frac{\lambda_1}{2}{\chi_1}^2 + \frac{1}{2}{z_1}^2 + \frac{1}{2}{z_3}^2 + \frac{1}{2}{z_5}^2 \tag{23}$$

Its derivative is

$$\dot{V}_5 = \lambda_1 \chi_1 z_1 + z_1 \dot{z}_1 + z_3 \dot{z}_3 + z_5 \dot{z}_5 \tag{24}$$

The resultant dynamics of z_3 is obtained as

$$\begin{aligned}\dot{z}_3 &= \dot{x}_3 - \dot{\alpha}_1(x_1) \\ &= \frac{1}{J_h}\left[\left(l_t S_f F_h(x_5)\cos\ x_2\right) - k_h x_3\right] - \frac{l_t S_f \cos\ x_2}{J_h}\alpha_3 + \frac{l_t S_f \cos\ x_2}{J_h}\alpha_3 - \frac{\partial \alpha_1}{\partial x_1}\dot{x}_1\end{aligned} \tag{25}$$

Therefore,

$$\dot{z}_3 = \frac{l_t S_f \cos\ x_2}{J_h}(F_h(x_5) - \alpha_3) - \frac{1}{J_h}(k_h x_3) - \frac{\partial \alpha_1}{\partial x_1}\dot{x}_1 + \frac{l_t S_f \cos\ x_2}{J_h}\alpha_3 \tag{26}$$

Substituting for $\alpha_3(x_1, x_3)$ from Eq. (21) in the last term on the right-hand side of Eq. (26) yields

$$\dot{z}_3 = \frac{l_t S_f \cos x_2}{J_h} z_5 - z_1 - c_3 z_3 \tag{27}$$

Also as
$\dot{z}_5 = \dot{F}_h(x_5) - \dot{\alpha}_3(x_1, x_3)$ and

$$\frac{dF_h}{dt} = \frac{dF_h}{d\omega_h}.\frac{d\omega_h(x_5)}{dt} = \frac{dF_h}{d\omega_h}.\frac{d\omega_h}{dx_5}.\frac{dx_5}{dt} = \frac{dF_h}{d\omega_h}.\dot{x}_5\frac{d\omega_h}{dx_5} \tag{28}$$

The dynamics of z_5 is obtained as

$$\dot{z}_5 = \frac{dF_h}{d\omega_h}.\frac{d\omega_h}{dx_5}.\frac{1}{T_{tr}}\ (u_h - x_5) - \dot{\alpha}_3(x_1, x_3) \tag{29}$$

Substituting Eqs. (18), (27) and (29) into Eq. (24) yields

$$\dot{V}_5 = -c_1 {z_1}^2 - c_3 {z_3}^2 + \ z_5\left[\frac{l_t S_f \cos x_2}{J_h} z_3 + \frac{dF_h}{d\omega_h}.\frac{d\omega_h}{dx_5}.\frac{1}{T_{tr}}\ (u_h - x_5) - \frac{\partial \alpha_3}{\partial x_1}\dot{x}_1 - \frac{\partial \alpha_3}{\partial x_3}\dot{x}_3\right] \tag{30}$$

To cancel out the nonlinear terms and stabilise the dynamics of z_5, the control input u_h is designed as

$$u_h = x_5 + \frac{T_{tr}}{\frac{dF_h}{d\omega_h}.\frac{d\omega_h}{dx_5}}\left(-\frac{l_t S_f \cos x_2}{J_h} z_3 + \frac{\partial \alpha_3}{\partial x_1}\dot{x}_1 + \frac{\partial \alpha_3}{\partial x_3}\dot{x}_3 - c_5 z_5\right) \tag{31}$$

So that,

$$\dot{V}_5 = -c_1 {z_1}^2 - c_3 {z_3}^2\ - c_5 {z_5}^2, \quad c_1, \quad c_3, \quad c_5\ > 0 \tag{32}$$

Evaluating the partial derivatives in Eq. (31) and expanding yields the control law for the HS

$$u_h = x_5 + \frac{T_{tr}}{\frac{dF_h}{d\omega_h}.\frac{d\omega_h}{dx_5}}\left\{-\frac{l_t S_f \cos x_2}{J_h}(x_3 + c_1 z_1 + \lambda_1 \chi_1 - \dot{x}_{1d}) + \frac{J_h}{l_t S_f \cos x_2}\left[-x_3(1 + \lambda_1 x_3 + c_3(c_1 + \lambda_1 z_1)) + \dot{x}_3\left(\frac{k_h}{J_h} - \lambda_1 z_1 - c_1 - c_3\right)\right] - c_5[F_h(x_5) - \alpha_3(x_1, x_3)]\right\} \tag{33}$$

3.2. Vertical subsystem integral backstepping

The decoupled model for the vertical subsystem (VS) of the TRMS [1] is obtained as

$$\begin{aligned}
\dot{x}_2 &= x_4 \\
\dot{x}_4 &= \frac{1}{J_v}\left[l_m S_f F_v(x_6) - k_v x_4 - G(x_2)\right] \\
\dot{x}_6 &= \frac{1}{T_{mr}}(u_v - x_6)
\end{aligned} \tag{34}$$

where $G(x_2) = g((A - \mathrm{B})\cos\ x_2 - \ C\sin x_2)$ is the return moment of the VS.
Let:

$$z_2 := x_2 - x_{2d} \tag{35}$$

$$z_4 := x_4 - \alpha_2 \tag{36}$$

$$z_6 := F_v(x_6) - \alpha_4 \tag{37}$$

where x_{2d} is the desired pitch angle, α_2 and α_4 are stabilising functions to be obtained in the backstepping design.

Step 1:

Select a CLF as

$$V_2 = \frac{\lambda_2}{2}{\chi_2}^2 + \frac{1}{2}{z_2}^2 \tag{38}$$

where $\chi_2 = \int_0^t z_2(\tau)d\tau$ and λ_2 is a positive constant.

Its derivative is

$$\dot{V}_2 = \lambda_2\chi_2\dot{\chi}_2 + z_2\dot{z}_2 = \lambda_2\chi_2 z_2 + \ z_2(\dot{x}_2 - \dot{x}_{2d}) \ = \lambda_2\chi_2 z_2 + z_2(x_4 - \dot{x}_{2d}) \tag{39}$$

Design the stabilising function $\alpha_2(x_2)$ by taking x_4 as the virtual control.

$$\alpha_2(x_2) = x_4 = -c_2 z_2 - \lambda_2\chi_2 + \dot{x}_{2d}, \quad c_2, \quad \lambda_2 \ > 0 \tag{40}$$

Hence,

$$\dot{V}_2 = -c_2{z_2}^2 \tag{41}$$

Step 2:

Select a CLF as

$$V_4 = \frac{\lambda_2}{2}{\chi_2}^2 + \frac{1}{2}{z_2}^2 + \frac{1}{2}{z_4}^2 \tag{42}$$

Its derivative is

$$\dot{V}_4 = \lambda_2\chi_2\dot{\chi}_2 + z_2\dot{z}_2 + z_4\dot{z}_4 \tag{43}$$

The resultant dynamics of z_2 is obtained as

$$\begin{aligned}\dot{z}_2 &= \dot{x}_2 = x_4 \\ &= x_4 - \alpha_2 + \alpha_2\end{aligned} \tag{44}$$

$$\dot{z}_2 = z_4 - c_2 z_2 - \lambda_2\chi_2 \tag{45}$$

With $\dot{z}_4 = \dot{x}_4 - \dot{\alpha}_2(x_2)$, the dynamics of $\dot{z}_4$ can be is expressed as

$$\dot{z}_4 \ = \frac{1}{J_v}\left[l_m S_f F_v(x_6) - G(x_2) - k_v x_4 \ \right] - \frac{\partial\alpha_2}{\partial x_2}\dot{x}_2 \tag{46}$$

Substituting Eqs. (45) and (46) into Eq. (43) yields

$$\dot{V}_4 = -c_2{z_2}^2 + z_4\left[z_2 + \frac{l_m S_f}{J_v}F_v(x_6) - \frac{1}{J_v}(G(x_2) + k_v x_4) - \frac{\partial\alpha_2}{\partial x_2}\dot{x}_2\right] \tag{47}$$

Taking $F_v(x_6)$ as the virtual control, $\alpha_4(x_2, x_4)$ is designed as

$$\alpha_4(x_2, x_4) = \frac{J_v}{l_m S_f}\left(-z_2 + \frac{1}{J_v}(G(x_2) + k_v x_4) + \frac{\partial \alpha_2}{\partial x_2}\dot{x}_2 - c_4 z_4\right) \tag{48}$$

Such that,

$$\dot{V}_4 = -c_2 {z_2}^2 - c_4 {z_4}^2, \quad c_2, c_4 > 0 \tag{49}$$

Step 3:
Finally a full state control law u_v to stabilise the entire VS is designed.
Select the CLF as

$$V_6 = \frac{\lambda_2}{2}{\chi_2}^2 + \frac{1}{2}{z_2}^2 + \frac{1}{2}{z_4}^2 + \frac{1}{2}{z_6}^2 \tag{50}$$

Its derivative is

$$\dot{V}_6 = \lambda_2 \chi_2 z_2 + z_2 \dot{z}_2 + z_4 \dot{z}_4 + z_6 \dot{z}_6 \tag{51}$$

The resultant dynamics of z_4 is obtained as

$$\begin{aligned} \dot{z}_4 &= \dot{x}_4 - \dot{\alpha}_2(x_2) \\ &= \frac{1}{J_v}\left[l_m S_f F_v(x_6) - G(x_2) - k_v x_4\right] - \frac{l_m S_f}{J_v}\alpha_4 + \frac{l_m S_f}{J_v}\alpha_4 - \frac{\partial \alpha_2}{\partial x_2}\dot{x}_2 \end{aligned} \tag{52}$$

Substituting for the positive α_4 term on the right-hand side of Eq. (50) yields

$$\dot{z}_4 = \frac{l_m S_f}{J_v} z_6 - z_2 - c_4 z_4 \tag{53}$$

Also as
$\dot{z}_6 = \dot{F}_v(x_6) - \dot{\alpha}_4(x_2, x_4)$ and

$$\frac{dF_v}{dt} = \frac{dF_v}{d\omega_v}.\frac{d\omega_v(x_6)}{dt} = \frac{dF_v}{d\omega_v}.\frac{d\omega_v}{dx_6}.\frac{dx_6}{dt} = \frac{dF_v}{d\omega_v}.\dot{x}_6\frac{d\omega_v}{dx_6} \tag{54}$$

the dynamics of $\dot{z}_6$ can be expressed as

$$\dot{z}_6 = \frac{dF_v}{d\omega_v}.\frac{d\omega_v}{dx_6}.\frac{1}{T_{mr}}(u_v - x_6) - \frac{\partial \alpha_4}{\partial x_2}\dot{x}_2 - \frac{\partial \alpha_4}{\partial x_4}\dot{x}_4 \tag{55}$$

Substituting Eqs. (45), (53) and (55) into Eq. (51) yields

$$\dot{V}_6 = -c_2 {z_2}^2 - c_4 {z_4}^2 + z_6\left[\frac{l_m S_f}{J_v} z_4 + \frac{dF_v}{d\omega_v}.\frac{1}{T_{mr}}(u_v - x_6)\cdot\frac{d\omega_v}{dx_6} - \frac{\partial \alpha_4}{\partial x_2}\dot{x}_2 - \frac{\partial \alpha_4}{\partial x_4}\dot{x}_4\right] \tag{56}$$

The control voltage u_v is designed as

$$u_v = x_6 + \frac{T_{mr}}{\frac{dF_v}{d\omega_v}.\frac{d\omega_v}{dx_6}}\left(-\frac{l_m S_f}{J_v} z_4 + \frac{\partial \alpha_4}{\partial x_2}\dot{x}_2 + \frac{\partial \alpha_4}{\partial x_4}\dot{x}_4 - c_6 z_6\right) \tag{57}$$

Such that,

$$\dot{V}_6 = -c_2 {z_2}^2 - c_4 {z_4}^2 - c_6 {z_6}^2, \quad c_2, c_4, c_6 > 0 \tag{58}$$

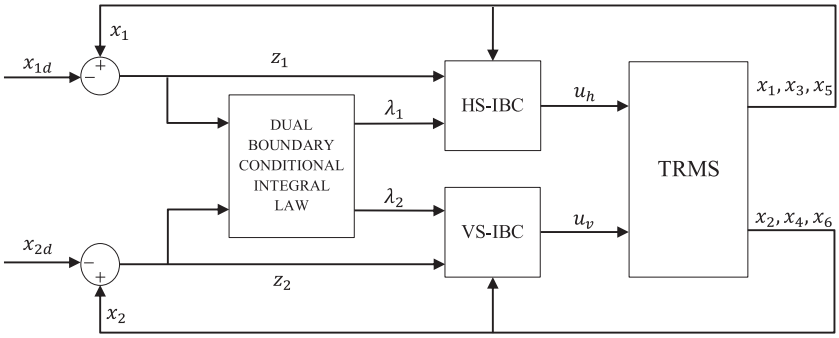

Fig. 3. TRMS with dual boundary conditional integral backstepping control (DBCIBC).

Evaluating the partial derivatives in Eq. (57) and expanding yields the final control law for the VS as

$$u_v = x_6 + \frac{T_{mr}}{\frac{dF_v}{d\omega_v}\cdot\frac{d\omega_v}{dx_6}}\left\{-\frac{l_m S_f}{J_v}(x_4 + c_2 z_2 + \lambda_2\chi_2 - \dot{x}_{2d}) + \frac{J_v}{l_m S_f}\left[x_4\left(-1 - \frac{g}{J_v}((A-B)\sin x_2 + C\cos x_2) - \lambda_2 x_4 - c_4(c_2 + \lambda_2 z_2)\right) + \dot{x}_4\left(\frac{k_v}{J_v} - c_2 - c_4 - \lambda_2 z_2\right)\right] - c_6[F_v(x_6) - \alpha_4(x_2, x_4)]\right\} \tag{59}$$

4. Dual boundary conditional integral law

In this section, the novel approach postulated by this paper to provide conditional integral action within two (outer and inner) boundary layers is introduced. For a simulation case with a constant reference signal and unmatched disturbances, the backstepping controller with analytical virtual control derivatives and no integral action is sufficient to guarantee zero steady state error. For a sinusoidal input reference however, obtaining zero tracking error is more challenging and requires integral action. In this work, the following integral gain law is formulated to minimise the tracking error without degrading the transient response.

$$\lambda_i(t) = \begin{cases} 0, & |z_i| > \mu_i > \delta_i \\ \lambda_{ri}, & \mu_i \geq |z_i| > \delta_i \\ \lambda_{ri} + k_{\lambda i}\int \mathrm{sgn}(\dot{x}_{id}(t).\ddot{x}_{id}(t))|z_i|\, dt, & |z_i| \leq \delta_i, \quad t < t_p \\ \lambda_{ri} + k_{\lambda i}\int |z_i|\, dt, & |z_i| \leq \delta_i, \quad t \geq t_p \end{cases} \tag{60}$$

For $i = 1$ and 2 and $0 \leq \lambda_i \leq \lambda_{mi}$ where $\lambda_{mi} \in R^+$ is the minimum integral gain required to achieve adequate tracking, μ_i and δ_i are the widths of the outer and inner boundary layers, respectively, $\lambda_{ri} < \lambda_{mi}$ is the integral gain within the outer boundary layer, $k_{\lambda i}$ is a positive constant and t_p is the time instant of the first peak in the reference input during the transient period. The closed loop system under the proposed DBCIBC scheme is shown in Fig. 3

Here, it is assumed that the reference is a bounded continuously differentiable signal of known frequency and the gains of the closed loop system c_i for $i = 1, 2, \ldots, 6$ without integral action, can be tuned such that the outputs of the HS and VS approach a neighbourhood of their respective reference signals. Within the outer boundary, integral action is then

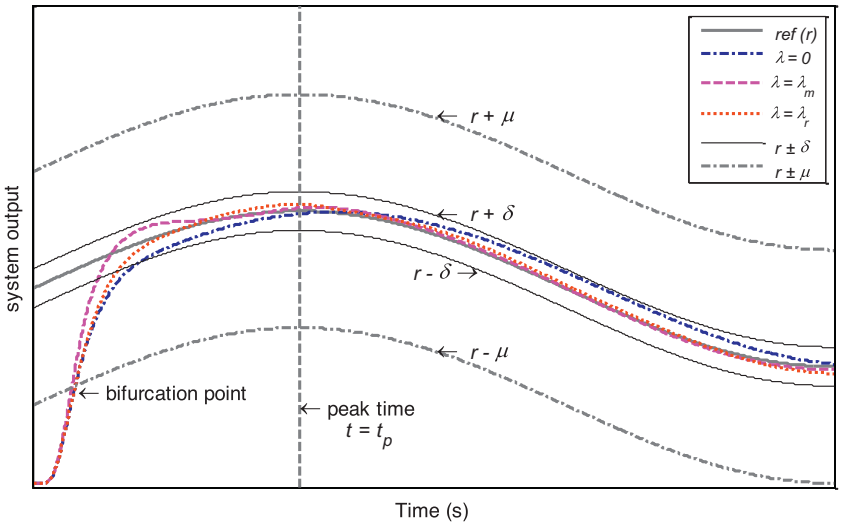

Fig. 4. Tuning of λ_m, λ_r, width of the outer boundary μ, width of the inner boundary, δ and integrator reset (peak) time.

applied to minimise the error by the integral gain law in Eq. (60) initially with $\lambda_i(t) = \lambda_{ri}$ which increases to λ_{mi} within the inner boundary at a rate determined by $k_{\lambda i}$. In the case of sinusoidal references, $\lambda_i(t)$ increases/decreases as determined by $\text{sgn}(\dot{x}_{id}(t).\ddot{x}_{id}(t))$ in Eq. (60) within the inner boundary when $t < t_p$ before increasing to λ_{mi} afterwards.

In general, consider a closed loop system with output $y(t)$ to a bounded reference $r(t)$ and continuous control law $u(t)$ augmented by a saturated integrator χ with integral gain $\lambda(t)$. Let $y_{\lambda_o}(t)$ be the output of the system with no integral action in the neighbourhood of $r(t)$ and $y_{\lambda_m}(t)$ be the output with sufficient integral action which adequately tracks $r(t)$ after a transient period. Assuming $|y(0)| > 0$, let μ and δ $(|y(0)| > \mu > \delta)$ be compact sets containing $r(t)$. A step by step procedure for tuning the integral gain law for this system is described in the following and shown in Fig. 4.

Tune all controller parameters using any known tuning process and determine λ_m as the minimum integral gain, such that the system output $y(t) = y_{\lambda_m}(t)$ precisely tracks the reference $r(t)$ after some transient period.

Set $\lambda = \lambda_o = 0$ and determine the bifurcation point y_b defined as the value of $y_{\lambda_o}(t)$ during the transient period where the output with sufficient integral action diverges from the output with no integral action i.e. $y_b := \max |y_{\lambda_o}||_{|y_{\lambda_m} - y_{\lambda_o}| \geq \varepsilon}$ where ε is a small positive constant.

Set the width of the outer boundary layer μ as the compact set containing y_b and $r(t)$.

Determine $\lambda_r < \lambda_m$ as the integral gain within the outer boundary that facilitates minimisation of the tracking error with marginal or no overshoot during the transient period.

Determine the width of the inner boundary layer δ as the compact set such that the response of step 4 above enters this boundary during the transient period and remains within it for all future time.

Tune k_λ to determine the rate at which $\lambda(t) = \lambda_r \rightarrow \lambda_m$ as a trade-off between overshoot and speed of convergence.

In the case of a sinusoidal reference, apply a reset once to the integrator χ at $t = t_p$ to further improve performance immediately after the first peak of the reference signal during the transient phase.

5. Stability of the TRMS under DBCIBC

In this section, the stability of the HS and VS of the TRMS with the system's uncertainties is analysed under the proposed control method.

5.1. Stability of the HS

The proposed control law in Eq. (33) with no integral action for the nominal HS as expressed in Eq. (7) ensures the negative definiteness of the Lyapunov derivative $\dot{V}_5$ in Eq. (32) which implies the exponential stability of the origin. The uncertainty in the HS form Eq. (1) is given as

$$\Delta f_h = J_h^{-1}\left(x_3 x_4 (D-E)\sin(2x_2) - J_{mr}\omega_m(x_6)x_4 \sin x_2 + \frac{J_{mr}}{T_{mr}}(u_v - x_6)\frac{d\omega_m(x_6)}{dx_6}\cos x_2\right) \tag{61}$$

and satisfies the extended matching condition i.e. it appears one integrator before the control input and only affects the dynamics of z_3 directly. Also $\Delta f_h\ (x_2, x_3, x_4, u_v)$ is bounded as x_3 and x_4 (the velocities of the beam in the HS and VS axes, respectively) are bounded since the nominal HS and VS are stabilised by the saturated control inputs u_v and u_h, respectively. The closed loop dynamics of the HS in the z coordinates from Eqs. (18), (27) and (29) with the uncertainty in Eq. (61) can be expressed in matrix form as

$$\dot{z}_h = \begin{bmatrix} -c_1 & 1 & 0 \\ -1 & -c_3 & \frac{l_t S_f \cos x_2}{J_h} \\ 0 & -\frac{l_t S_f \cos x_2}{J_h} & -c_5 \end{bmatrix} z_h + \begin{bmatrix} -\lambda_1\chi_1 \\ \Delta f_h \\ 0 \end{bmatrix} \tag{62}$$

where $z_h = [z_1 \quad z_3 \quad z_5\ ]^T$

Let

$$V_h = \frac{\lambda_1}{2}{\chi_1}^2 + \frac{1}{2}{z_h}^T z_h \tag{63}$$

The derivative of V_h along the dynamics of z_h is obtained as

$$\dot{V}_h = -\sum_{i=1,\ 3,\ 5} c_i {z_i}^2 + z_3\Delta f_h \ \leq\ -2\min(c_i)\frac{1}{2}{z_h}^T z_h + z_3\Delta f_h \tag{64}$$

or

$$\dot{V}_h \leq -\min(c_h)\|z_h\|^2 + |z_3\Delta f_h| \tag{65}$$

where $c_h = [c_1\ c_3\ c_5]$

It is assumed there exists a bounded positive constant p_h such that

$$p_h\|z_h\|^2 \ \geq |z_3\Delta f_h|, \quad \forall\ t \geq 0$$

This assumption is valid as $\Delta f_h\ (x_2, x_3, x_4, u_v)$ is bounded. Moreover, the first term in the parenthesis on the right of Eq. (61) vanishes at the origin, the second term has a low upper bound (owing to J_{mr}) and the third term is exponentially decaying.

Theorem 1. If $\min(c_h) > p_h$ then the HS of the TRMS will be globally asymptotically stable for the control law proposed in Eq. (33) and with λ_1 defined by Eq. (60) for the outer and inner boundary layers μ_1 and δ_1, respectively.

Proof. For the simulation case of a constant reference signal with unmatched disturbances, $\lambda_1 = 0$ and the controller is reduced to a backstepping controller with no integral action. Calculating the derivative of V_h along the closed loop trajectories of the HS yields

$$\dot{V}_h \leq -\min(c_h)\|z_h\|^2 + |z_3 \Delta f_h| \ < 0 \tag{66}$$

Thus the system is exponentially stable for the proposed control input in Eq. (33). In the case of a sinusoidal reference signal, integral action is provided conditionally as expressed by Eq. (60) and the system is analysed in three regions of interest:

Region 1: $|z_1| > \mu_1 > \delta_1$

The tracking error lies in the exterior of the outer boundary layer and $\lambda_1 = 0$. This leads to the same controller as in the case of a constant reference signal and the magnitude of the tracking error $|z_1|$ will decrease exponentially into region 2.

Region 2: $\mu_1 \geq |z_1| > \delta_1$

The tracking error lies between the two boundary layers and the integral gain $\lambda_1 = \lambda_{r1}$. The derivative of V_h along the closed loop trajectories of the HS now becomes

$$\dot{V}_h \leq -\min(c_h)\|z_h\|^2 + |z_3 \Delta f_h| \ \leq \ 0 \tag{67}$$

which is only negative semi-definite. Since $\dot{V}_h$ is nonpositive, it can be concluded that z_1, z_3, z_5 and χ_1 are bounded. This implies that the derivatives of the error signals are also bounded i.e. $\dot{z}_1, \dot{z}_2, \dot{z}_3 \in L_\infty$. Also, from the expression of the Lyapunov function derivative in Eq. (32) $z_1, z_3, z_5, \in L_2$ and it can be deduced from Barbalat's lemma that the closed-loop system will be asymptotically stable for the proposed control input u_h in Eq. (33). That is $\lim_{t\to\infty} z_5, z_3, z_1 = 0$.

Region 3: $|z_1| \leq \delta_1$

In this region, the integral law in Eq. (60) prevents λ_1 from changing instantaneously and the same argument for region 2 applies. The integrator χ_1 is reset to zero once in this region at time instant $t = t_p$. The Lyapunov function for the system at this instant is

$$V_{5r}(t) = \frac{1}{2}{z_1}^2 + \frac{1}{2}{z_3}^2 + \frac{1}{2}{z_5}^2 < \ V_h(t)$$

This leads to a negative jump in the Lyapunov function which ensures $\dot{V}_{5r} \leq 0$ and not only preserves the stability of the system [33] but also improves the transient performance after the integrator reset [34].

5.2. Stability of the VS

The Lyapunov derivative $\dot{V}_6$ in Eq. (58) for the nominal VS as expressed in Eq. (34) is rendered negative definite by the proposed control law in Eq. (59) with no integral action.

As such, the origin of the VS is also exponential stable. The uncertainty in the VS from Eq. (1) is given as

$$\Delta f_v = J_v^{-1}\left(-0.0252{x_3}^2 \sin(2x_2) + \frac{J_{tr}}{T_{tr}}(u_h - x_5)\frac{d\omega_t(x_5)}{dx_5}\right) \tag{68}$$

The closed loop dynamics of the VS in the z coordinates from Eqs. (45), (53) and (55) with the uncertainty in Eq. (68) can be expressed as

$$\dot{z}_v = \begin{bmatrix} -c_2 & 1 & 0 \\ -1 & -c_4 & \frac{l_m S_f}{J_v} \\ 0 & -\frac{l_m S_f}{J_v} & -c_6 \end{bmatrix} z_v + \begin{bmatrix} -\lambda_2 \chi_2 \\ \Delta f_v \\ 0 \end{bmatrix} \tag{69}$$

where $z_v = [z_2 \quad z_4 \quad z_6]^T$

Let

$$V_v = \frac{\lambda_2}{2}{\chi_2}^2 + \frac{1}{2}{z_v}^T z_v \tag{70}$$

The derivative of V_v along the dynamics of z_v is obtained as

$$\dot{V}_v = -\sum_{i=2,4,6} c_i {z_i}^2 + z_4 \Delta f_v \leq -\min(c_v)\|z_v\|^2 + |z_4 \Delta f_v| \tag{71}$$

where $c_v = [c_2 \; c_4 \; c_6]$

It is assumed there exists a bounded positive constant p_v such that

$$p_v \|z_v\|^2 \geq |z_4 \Delta f_v|, \quad \forall\, t \geq 0$$

This assumption is justified as $\Delta f_v(x_2, \quad x_3, u_h)$ is bounded.

Theorem 2. If $\min(c_v) > p_v$ then the VS of the TRMS will be globally asymptotically stable for the control law proposed in Eq. (59) and with λ_2 defined by Eq. (60) for the outer and inner boundary layers μ_2 and δ_2, respectively.

Proof. For the simulation case of a constant reference signal $\lambda_2 = 0$ and the controller is reduced to a backstepping controller with no integral action. Also, the pitch angle is physically restrained to $-\pi/2 < x_2 < \pi/2$. Calculating the derivative of V_v along the closed loop trajectories of the VS yields

$$\dot{V}_v = -\min(c_v)\|z_v\|^2 + |z_4 \Delta f_v| < 0 \tag{72}$$

Thus the system is exponentially stable for the proposed control input in Eq. (59). For a sinusoidal reference signal, conditional integral action is provided by the gain law expressed in Eq. (60) and the system is analysed in three regions as below:

Region 1: $|z_2| > \mu_2 > \delta_2$

The tracking error $|z_2|$ is external the outer boundary layer and $\lambda_2 = 0$. This leads to the same stable controller as in the case of a constant reference signal and the magnitude of the tracking error z_2 will decrease exponentially into region 2.

Region 2: $\mu_2 \geq |z_2| > \delta_2$

The tracking error is situated between the two boundary layers and the integral gain $\lambda_2 = \lambda_{r2}$. The derivative of V_v along the systems trajectories becomes

$$\dot{V}_v = -\min(c_v)\|z_v\|^2 + |z_4 \Delta f_v| \leq 0 \tag{73}$$

Since $\dot{V}_v$ is nonpositive, it can also be concluded from Barbalat's lemma that the closed-loop system will be asymptotically stable for the proposed control input in Eq. (59). That is $\lim_{t\to\infty} z_6, z_4, z_2 = 0$.

Region 3: $|z_2| \leq \delta_2$

In this region, the integral law in Eq. (60) prevents λ_2 from changing abruptly and the same argument for region 2 applies. The integrator χ_2 is reset to zero once in this region at time instant $t = t_p$. The Lyapunov function for the system now becomes

$$V_{6r}(t) = \frac{1}{2}z_2{}^2 + \frac{1}{2}z_4{}^2 + \frac{1}{2}z_6{}^2 < V_v$$

This leads to a negative jump in the Lyapunov function which ensures $\dot{V}_{6r} \leq 0$ thereby preserving system stability and improving the transient performance after the integrator reset.

6. Simulation results

The designed controllers for the HS (yaw) and VS (pitch) are tested by simulation in 2-DOFs using three different reference inputs. Step, square-wave and sine-wave inputs are applied to each subsystem for a duration of 50 s. Tracking error and control signal indices are used to assess the performance of the controllers. Both indices are defined as the sum of their absolute values from 0 to 50 s and computed at a sample time of 0.05 s. Lower indices indicate better tracking performance and less control energy. For assessing the transient response characteristics, the rise time is defined as the time the response takes to rise from 10% to 90% of the steady-state value and a threshold of 5% for the settling time. The closed loop system is implemented in Simulink using the *ode5* solver with a fixed-step size of 0.01 s.

6.1. Controller parameters and reference inputs

The backstepping controller parameters for the HS are heuristically set at $c_1 = 1.35$, $c_3 = 7.0$ and $c_5 = 2$. The integral law parameters are set at $\lambda_{r1} = 1.7$, $\lambda_{m1} = 3.0, k_{\lambda 1} = 20$ with the integrator χ_1 and control signal saturated u_h at $\pm$ 0.1 and $\pm$ 0.5, respectively. The widths of the outer and inner boundary regions are, respectively set at $\mu_1 = 0.3$ and $\delta_1 = 0.03$. The controller is implemented using state feedback for x_1, x_3 and x_5. However $\dot{x}_3$ is calculated from the values of the feedback states according to its expression in Eq. (7). The HS is tested with: (i) a step setpoint of 1.0 rad, (ii) a square-wave reference with amplitude of 0.5 rad and period of 40 s and (iii) a sine-wave with amplitude of 0.5 rad and period of 40 s.

In the case of the VS, the backstepping controller parameters are heuristically set at $c_2 = 1.31$, $c_4 = 6.45$ and $c_6 = 1.86$. The integrator χ_2 is saturated at $\pm$ 0.1 and the control signal u_v is limited between 0 and 1. The integral gain law parameters are set at $\lambda_{r2} = 0.5$, $\lambda_{m2} = 2.0, k_{\lambda 2} = 20$ with the widths of the boundary layers set at $\mu_2 = 0.3$ and $\delta_2 = 0.03$. The controller is implemented using state feedback for x_2, x_4 and x_6 and $\dot{x}_4$ is calculated from x_4 and x_6 according to its expression in Eq. (34). The input signals applied to the VS are: (i) a step setpoint input of 0.2 rad, (ii) a square-wave input of 0.2 rad amplitude and period of 40 s and (iii) a sine-wave reference of amplitude 0.2 rad and period of 40 s.

Fig. 5 shows the responses of the system to a step input. It can be observed that the outputs of the cross coupled system settle quickly at their respective setpoints without overshooting. The superimposed plot of the normalised control signal also indicates smooth

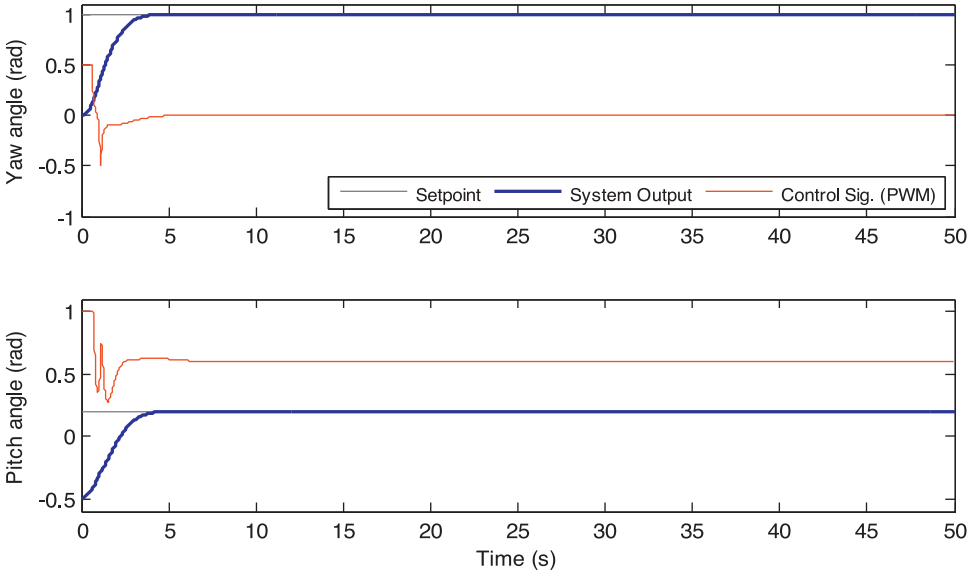

Fig. 5. Step response of the TRMS with DBCIBC.

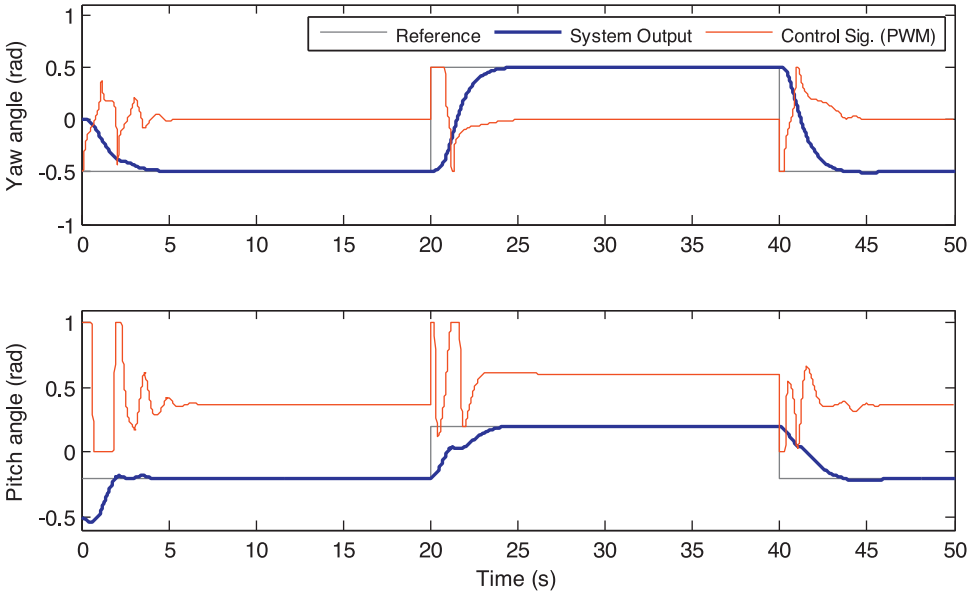

Fig. 6. Square-wave response of the TRMS with DBCIBC.

operation and practicality of the controller. The responses to a square-wave input are shown in Fig. 6 where it can be seen that the system responds quickly to simultaneous step changes in the reference signals.

The tracking responses to sine-wave reference inputs are shown in Fig. 7. Both the HS and VS show excellent tracking and transient response behaviour as a result of the dual

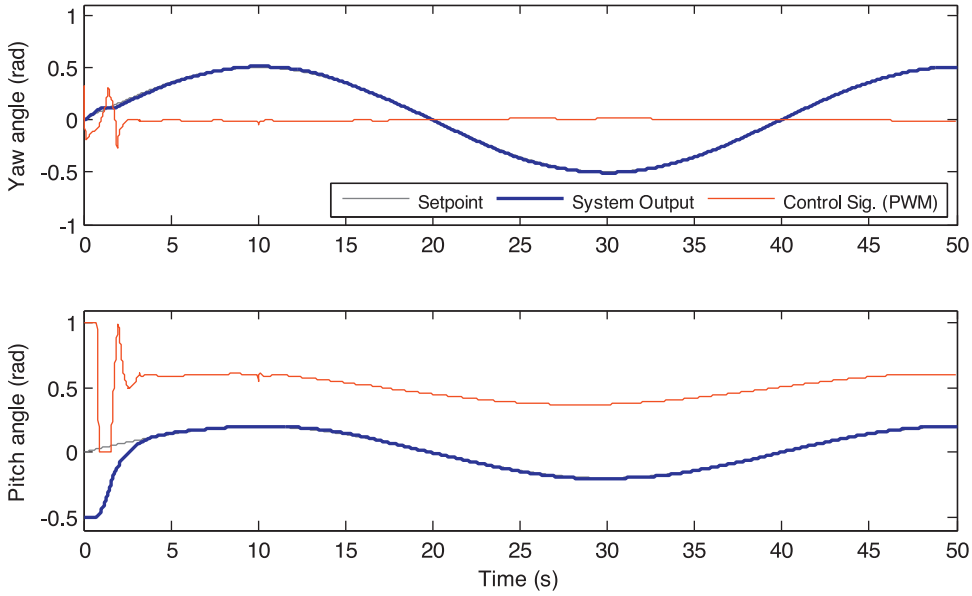

Fig. 7. Sine-wave response of the TRMS with DBCIBC.

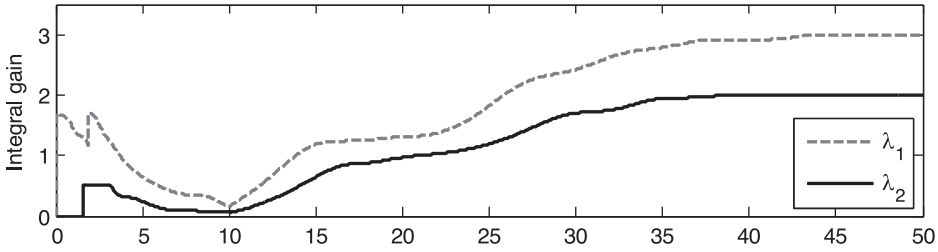

Fig. 8. Integral gains of the HS and VS with sine-wave reference.

boundary conditional integral law. It can be noticed that the HS starts within the inner boundary region and remains there for all future time after the short transient period. The VS however has initial conditions exterior to the outer boundary region but nonetheless, the controller acts to track the reference with a quick rise time and without overshoot. A slight dip in the value of the control signals at 10 s in both plots is due to the integrator resets.

Fig. 8 shows the plots of the variable integral gains for the HS and VS as a result of the integral law which facilitates excellent tracking ability whilst maintaining a good transient response. Form Fig. 8, it is seen that λ_2 has an initial value of 0 as the output lies exterior to the outer boundary layer. On reaching the outer boundary, constant integral action with a gain of $\lambda_2 = \lambda_{r2} = 0.5$ is applied which enables tracking without overshoot and helps to propel the output into the inner boundary. Once the inner boundary is reached, the integral gain is reduced at a rate proportional to the error signal to prevent overshoot. This continues until the reference peaks where the integral law reverses the trend and increases the integral gain until it reaches the allowed maximum, enabling adequate tracking after the transient period.

Table 2
TRMS error indices with M-RGA, FSFISC, SOSMC and DBCIBC.

Reference		Error index			
		M-RGA [2]	FSFISC [15]	SOSMC [16]	DBCIBC
Step	HS	54.52	35.11	45.23	31.25
	VS	27.46	28.81	23.08	24.77
Square	HS	134.03	82.11	83.70	79.61
	VS	90.21	43.16	45.80	36.25
Sine	HS	20.92	6.17[a]	32.33	5.52
	VS	52.61	49.11[a]	42.20	21.81

[a]Given for a 50 s period reference signal.

Table 3
TRMS control indices with M-RGA, FSFISC, SOSMC and DBCIBC.

Reference		Control index			
		M-RGA [2]	FSFISC [15]	SOSMC [16]	DBCIBC
Step	HS	40.47	11.64	12.45	12.82
	VS	617.10	600.00	645.98	605.43
Square	HS	165.32	42.93	42.34	43.74
	VS	551.59	465.54	487.29	467.83
Sine	HS	18.93	7.27[a]	10.68	13.00
	VS	501.78	488.48[a]	515.42	504.44

[a]Given for a 50 s period reference signal.

The integral gain λ_1 for the HS also shows a similar pattern of behaviour only that in this case, it starts with an initial value of $\lambda_1 = \lambda_{r1} = 1.7$ since the HS has zero initial conditions and begins within the inner boundary. The integral gain reduces slightly and returns to its initial value as a result of the undamped HS exiting the inner boundary after about 2 s. The HS however immediately re-enters the boundary and the integral gain behaves similarly to that of the VS.

Tables 2 and 3, respectively, summarise the error and control indices of the DBCIBC for step, sine and square-wave inputs. Also shown are the indices of the controllers proposed for the system in [2,15,16] for comparisons.

It is quite clear that the DBCIBC outperforms the M-RGA PID controller, having much better error and control signal indices for all input waveforms. The performance of the DBCIBC also exceeds that of the SOSMC in the case of a square-wave and especially for a sine-wave input. Although the SOSMC controller performs slightly better than the DBCIBC for a step reference in the VS, this is achieved at the expense of a disproportionately larger control effort as shown in Table 3. The DBCIBC also generally has much better error indices when compared to the FSFISC (a sliding mode controller with a fuzzy compensator) albeit with slightly higher control effort for step and square input waveforms. In the case of the sine-wave input however, the DBCIBC clearly outperforms the FSFISC, reducing the error index in the VS by over 50%. It is also worth mentioning that the indices for a sine-wave input of the FSFISC in [15] were obtained using a reference signal with a longer time period (50 s) which is easier to track and results in lower indices. The improvement in sine-wave

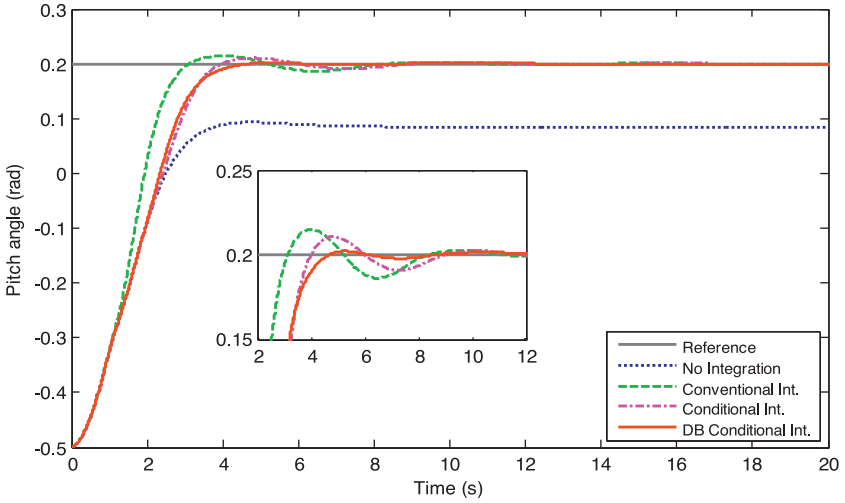

Fig. 9. 2-DOF step response of the perturbed VS under backstepping with no integration, conventional integration, conditional integration ($\mu = 0.3$) and DB conditional integration ($\mu_2 = 0.35$, $\delta_2 = 0.03$).

Table 4
Comparison of different integration techniques on the perturbed vs for a step input.

Integration type	Rise time	Settling time	Overshoot (%)	Error index	Control index
None	–	–	–	133.24	641.38
Conventional	1.83	2.65	2.12	22.74	832.45
Conditional	2.52	3.39	1.51	26.30	827.94
DB Conditional	2.43	3.37	0.30	25.49	828.77

tracking without degrading the transient response by the uncompensated DBCIBC is achieved by means of the dual boundary conditional integral law.

6.2. Transient response improvement

To study the effectiveness of the DBCIBC in improving the transient performance characteristics, the response of the VS (which has initial conditions exterior to the outer boundary layer) is examined under no integration, conventional integration, conditional integration and the proposed dual boundary conditional integration for step and sine-wave inputs.

For a step input, the VS is perturbed by increasing the return moment $G(x_2)$ by a factor of 1.21 such that a steady state error (as will occur in a practical case) appears in the pitch angle response which requires a minimum integral gain of $\lambda_2 = 2.0$ to eliminate. Fig. 9 shows the 2-DOF step response of the VS under backstepping control with different integration approaches.

It is clear that the integral action is required to eliminate the error in the system and doing so by conventional means i.e. when integral action is applied at time $t = 0$, leads to undesired overshoot and oscillation. Table 4 summarises the transient characteristics and error and control indices obtained using all the approaches. It can be observed that application of conditional integration with the width of the boundary μ at 0.3 is able to reduce the overshoot from 2.12% to 1.51%. However, with the proposed dual boundary conditional

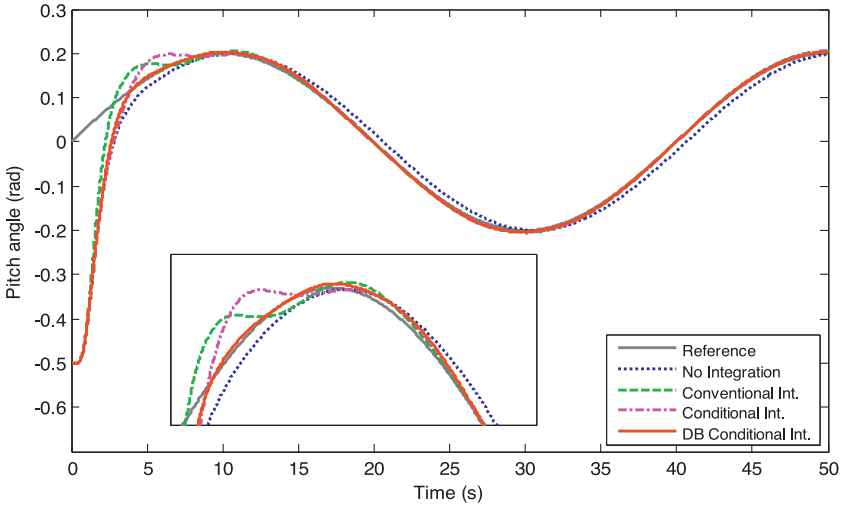

Fig. 10. 1-DOF sine-wave tracking response of the VS under backstepping control with different integration approaches.

Table 5
Comparison of different integration techniques on the vs for a sinusoidal reference input.

Integration type	Rise time	Settling time	Overshoot (%)	Error index	Control index
None	3.38	4.36	4.23	32.47	502.53
Conventional	2.37	5.41	8.72	21.69	506.93
Conditional	3.18	6.60	7.81	24.44	505.21
DB Conditional	2.94	3.28	1.61	21.76	504.48

integration method with $\mu_2 = 0.35$ and $\delta_2 = 0.03$, the overshoot (0.3%) is virtually eliminated. This is achieved despite that the width of the outer boundary is larger than the width of the boundary in the case of conditional integration. In addition, Table 4 indicates that the rise time, settling time and error index are also improved with similar control effort when compared to the conditional integration case.

For a sine-wave input, the 1-DOF response of the unperturbed VS is sufficient to demonstrate the effectiveness of the DBCIBC in improving transient performance. Fig. 10 shows the responses with different integration appraches with the transient characteristics and error and control indices given in Table 5. From the responses, it can be observed that the output with no integration attempts to track the reference but effectively has a time lag. The output with conventional integration ($\lambda_2 = 1.1$) tracks the reference but displays a poor transient response due to overshooting and a longer settling time. The output with conditional integration ($\lambda_2 = 1.0, \mu = 0.3$) also tracks the reference but overshoots and has a slower rise time than that of conventional integration. As such, for a sinusoidal reference, conditional integration does not show significant improvement in the transient response as compared to conventional integration.

The output of the dual boundary conditional integration ($\mu_2 = 0.3$, $\delta_2 = 0.03$) combines the best of both worlds by tracking the reference with faster rise time than the conditional case with negligible overshoot, leading to a reduction of over 30% in the settling time as compared to the other methods. Table 5 also shows that the dual boundary conditional method has a comparable error index with the conventional method achieved with similar control effort.

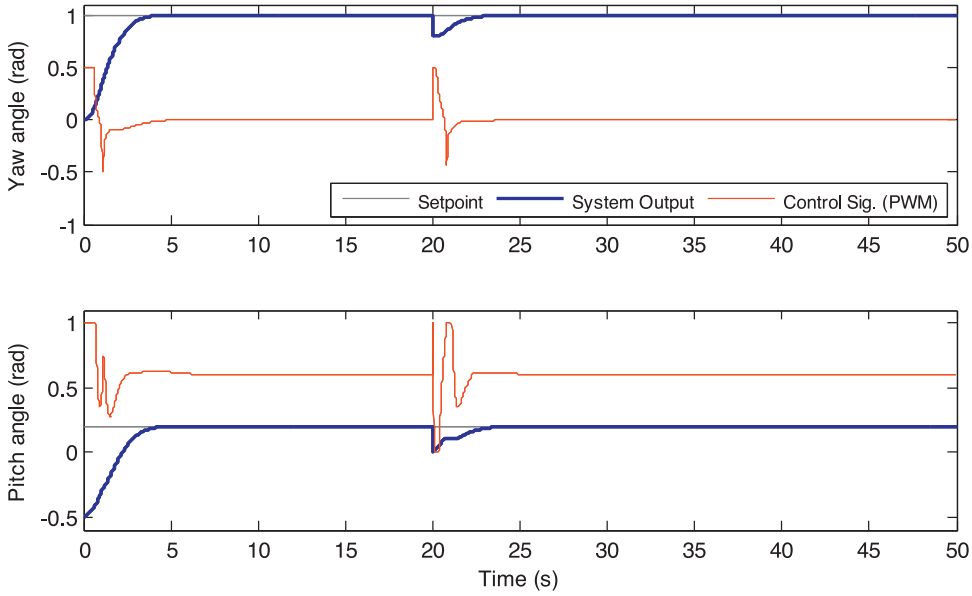

Fig. 11. Step response of the TRMS with DBCIBC subjected to an external disturbance.

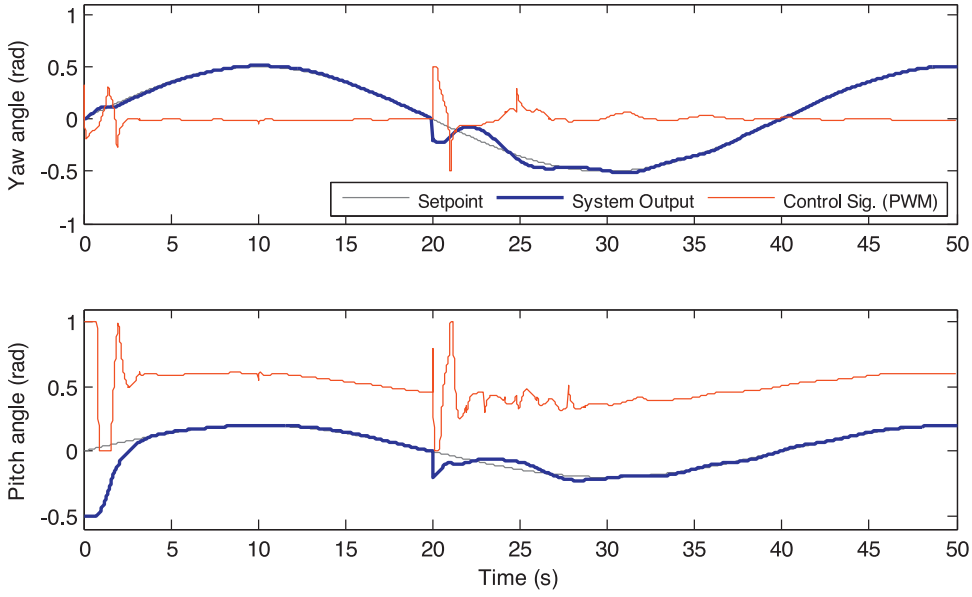

Fig. 12. Sine-wave response of the TRMS with DBCIBC subjected to an external disturbance.

6.3. Robustness

The robustness properties of the system under the proposed control method are tested by application of an external disturbance of −0.2 rad at 20 s to each subsystem. Figs. 11 and 12, respectively, show the responses of system under the disturbance with step and sine-wave input

references. It can be seen for both the HS and VS, the controller is able to handle the external disturbance. This however, as expected, takes longer time in the case of the sine-wave input.

7. Conclusion

A novel conditional integration method with dual boundaries and an adaptation gain mechanism in combination with integral backstepping control has been described in this paper. The designed DBCIBC has been applied to the TRMS and guarantees the stability of the system in the presence of uncertainties and external disturbances. The main result differentiates from the existing body of literature in that the proposed method achieves efficient and robust trajectory tracking while simultaneously improving the transient performance characteristics of the system under strong cross coupling effects. Comparisons with previously proposed control methods also show that the DBCIBC gives better performance in terms of tracking error and control signal indices especially for the more difficult task of tracking a time varying waveform.

References

[1] Feedback corporation, Twin Rotor MIMO System 33–220 User Manual, Feedback Instruments Co., East Sussex, UK, 1998.
[2] J.G. Juang, M.T. Huang, W.K. Liu, PID control using presearched genetic algorithms for a MIMO system, IEEE Trans. Syst. Man Cybern. Part C 38 (2008) 716–727 (Applications and Reviews).
[3] F.M. Aldebrez, M.S. Alam, M.O. Tokhi, Input-shaping with GA-tuned PID for target tracking and vibration reduction, in: Proceedings of the IEEE International Symposium on Intelligent Control, and Mediterrean Conference on Control and Automation, Limassol, Cyprus, 2005, pp. 485–490.
[4] P. Wen, T.W. Lu, Decoupling control of a twin rotor mimo system using robust deadbeat control technique, IET Control Theory Appl. 2 (2008) 999–1007.
[5] S.M. Ahmad, A.J. Chipperfield, M.O. Tokhi, Dynamic modeling and optimal control of a twin rotor MIMO system, in: Proceedings of the IEEE National Aerospace and Electronics Conference, Dayton, Ohio, USA, 2000, pp. 391–398.
[6] B. Pratap, A. Agrawal, S. Purwar, Optimal control of twin rotor MIMO system using output feedback, in: Proceedings of the 2nd International Conference on Power, Control and Embedded Systems (ICPCES), Allahabad, India, 2012, pp. 1–6.
[7] A. Phillips, F. Sahin, Optimal control of a twin rotor MIMO system using LQR with integral action, in: Proceedings of the World Automation Congress (WAC), Hawai'i, USA, 2014, pp. 114–119.
[8] A. Rahideh, M.H. Shaheed, Stable model predictive control for a nonlinear system, J. Frankl. Inst. 348 (2011) 1983–2004.
[9] B.U. Islam, N. Ahmed, D.L. Bhatti, S. Khan, Controller design using fuzzy logic for a twin rotor MIMO system, in: Proceedings of the 7th International Multi Topic Conference (INMIC), Islamabad, Pakistan, 2003, pp. 264–268.
[10] A. Rahideh, M.H. Shaheed, Hybrid fuzzy-PID-based control of a twin rotor MIMO system, in: Proceedings of the 32nd Annual Conference on IEEE Industrial Electronics, Paris, France, 2006, pp. 48–53.
[11] C.W. Tao, J.S. Taur, Y.C. Chen, Design of a parallel distributed fuzzy LQR controller for the twin rotor multi-input multi-output system, Fuzzy Sets Syst. 161 (2010) 2081–2103.
[12] J. Su, C. Liang, H. Chen, Robust control of a class of nonlinear systems and its application to a twin rotor MIMO system, in: Proceedings of the IEEE International Conference on Industrial Technology, 2, Bangkok, Thailand, 2002, pp. 1272–1277.
[13] Ahmed, A.I. Bhatti, S. Iqbal, Nonlinear robust decoupling control design for twin rotor system, in: Proceedings of the 7th Asian Control Conference, Hong Kong, 2009, pp. 937–942.
[14] D.K. Saroj, I. Kar, V.K. Pandey, Sliding mode controller design for twin rotor MIMO system with a nonlinear state observer, in: Proceedings of the International Multi-Conference on Automation, Computing, Communication, Control and Compressed Sensing (iMac4s), Kerala, India, 2013, pp. 668–673.
[15] C.W. Tao, J.S. Taur, Y.H. Chang, C.W. Chang, A novel fuzzy-sliding and fuzzy-integral-sliding controller for the twin-rotor multi-input multi-output system, IEEE Trans. Fuzzy Syst. 18 (2010) 893–905.

[16] S. Mondal, C. Mahanta, Adaptive second-order sliding mode controller for a twin rotor multi-input-multi-output system, IET Control Theory Appl. 6 (2012) 2157–2167.
[17] M. Lopez-Martinez, C. Vivas, M.G. Ortega, A multivariable nonlinear H-Infinity controller for a laboratory helicopter, in: Proceedings of the Joint 44th IEEE and European Control Conference on Decision and Control, Seville, Spain, 2005, pp. 4065–4070.
[18] M. Saeki, J.I. Imura, Y. Wada, Flight control design and experiment of a twin rotor helicopter model via 2 step exact linearization, in: Proceedings of the 1999 IEEE International Conference on Control Applications, 141, Hawa'i, USA, 1999, pp. 146–151.
[19] M. Lopez-Martinez, J.M. Diaz, M.G. Ortega, F.R. Rubio, Control of a laboratory helicopter using switched 2-step feedback linearization, in: Proceedings of the 2004 American Control Conference, 5, Boston, USA, 2004, pp. 4330–4335.
[20] F.Nejjari Rotondo, V. Puig, Quasi-LPV modeling, identification and control of a twin rotor MIMO system, Control Eng. Pract. 21 (2013) 829–846.
[21] A. Isidori, C.I. Byrnes, Output regulation of nonlinear systems, IEEE Trans. Autom. Control 35 (1990) 131–140.
[22] R.A. Freeman, P.V. Kokotovic, Optimal nonlinear controllers for feedback linearizable systems, in: Proceedings of the 1995 American Control Conference, 4, Seattle, Washington, USA, 1995, pp. 2722–2726.
[23] S. Seshagiri, H.K. Khalil, Robust output feedback regulation of minimum-phase nonlinear systems using conditional integrators, Automatica 41 (2005) 43–54.
[24] A. Singh, H.K. Khalil, Regulation of nonlinear systems using conditional integrators, Int. J. Robust Nonlinear Control 15 (2005) 339–362.
[25] B. Hunnekens, N.v.d. Wouw, M. Heertjes, H. Nijmeijer, Synthesis of variable gain integral controllers for linear motion systems, IEEE Trans. Control Syst. Technol. 23 (2015) 139–149.
[26] R. Skjetne, T.I. Fossen, On integral control in backstepping: analysis of different techniques, in: Proceedings of the 2004 American Control Conference, 2, Boston, Massachusetts, 2004, pp. 1899–1904.
[27] D. Sheng, Y. Wei, S. Cheng, J. Shuai, Adaptive backstepping control for fractional order systems with input saturation, J. Frankl. Inst., 354(2017) 2245–2268.
[28] I. Kanellakopoulos, P.T. Krein, Integral-action nonlinear control of induction motors, in: Proceedings of the 12th IFAC World Congress, Sydney, Australia, 1993, pp. 251–254.
[29] R. Rashad, A. Aboudonia, A. El-Badawy, A novel disturbance observer-based backstepping controller with command filtered compensation for a MIMO system, J. Frankl. Inst. 353 (2016) 4039–4061.
[30] T. Yaolong, C. Jie, T. Hualin, H. Jun, Integral backstepping control and experimental implementation for motion system, in: Proceedings of the 2000 IEEE International Conference on Control Applications, Anchorage, Alaska, USA, 2000, pp. 367–372.
[31] M. Krstic, I. Kanellakopoulos, P.V. Kokotovic, Nonlinear and Adaptive Control Design, Wiley, 1995.
[32] Z. Ding, Nonlinear and adaptive control systems, IET, London, 2013.
[33] M.S. Branicky, Multiple Lyapunov functions and other analysis tools for switched and hybrid systems, IEEE Trans. Autom. Control 43 (1998) 475–482.
[34] J. Bakkeheim, T.A. Johansen, Ø.N. Smogeli, A.J. Sorensen, Lyapunov-based integrator resetting with application to marine thruster control, IEEE Trans. Control Syst. Technol. 16 (2008) 908–917.